DEVELOPMENT OF A QUANTITATIVE ASSAY TO DISTINGUISH GLAUCOMA-CAUSING AND BENIGN OLFACTOMEDIN VARIANTS

A Thesis
Presented to
The Academic Faculty

by

Joyce Nicole Burns

In Partial Fulfillment
of the Requirements for the Degree
Master of Science in the
School of Chemistry and Biochemistry

Georgia Institute of Technology
December 2010

DEVELOPMENT OF A QUANTITATIVE ASSAY TO DISTINGUISH GLAUCOMA-CAUSING AND BENIGN OLFACTOMEDIN VARIANTS

Approved by:

Dr. Raquel Lieberman, Advisor
School of Chemistry and Biochemistry
Georgia Institute of Technology

Dr. Wendy L. Kelly
School of Chemistry and Biochemistry
Georgia Institute of Technology

Dr. Nils Kröger
School of Chemistry and Biochemistry
Georgia Institute of Technology

Date Approved: November 15, 2010

ACKNOWLEDGEMENTS

I would like to thank Dr. Raquel Lieberman for her support and guidance in my research. I would also like to thank Dr. Derrick Watkins, Susan Orwig, Julia Harris, Chandler Walker, and Katherine Turnage for their individual contributions to the research presented in this thesis. Thank you to the Hud lab for allowing the use of their CD spectropolarimeter and to the Institute of Biotechnology and Biosciences core facility for RT-PCR access. Finally, thank you to everyone in the Lieberman group for their support and advice. This work was supported by grants provided by the Glaucoma Research Foundation and the American Health Assistance Foundation National Glaucoma Research program awarded to Dr. Raquel Lieberman.

TABLE OF CONTENTS

Page

ACKNOWLEDGEMENTS iii

LIST OF TABLES v

LIST OF FIGURES vi

LIST OF SYMBOLS AND ABBREVIATIONS vii

SUMMARY viii

CHAPTER

1 Protein Expression and Purification 1

Introduction 1

Expression and Purification of Wild-type MBP-OLF 4

Expression and Purification of Mutant MBP-OLFs 8

Expression and Purification of Full-length Myocilin 9

2 Development of a Quantitative Assay 13

3 Biophysical Characterization 28

Circular Dichroism 28

Thioflavin T Assay 31

Propensity of Aggregation in Size-Exclusion Chromatography 33

4 Methods and Materials 36

APPENDIX A: List of Primers 41

REFERENCES 43

LIST OF TABLES

Page

Table 1: Peptides identified via mass spectrometry from full myocilin 12

Table 2: Effect of osmolytes on T_m of OLF and mutants 22

Table 3: Compilation of data on myocilin variants from this and previous studies 24

Table 4: Fluorescence intensity in the presence of thioflavin T at 485 nm 32

LIST OF FIGURES

	Page
Figure 1: Myocilin Sequence	2
Figure 2: OLF Purification	7
Figure 3: Purification of Full-length Myocilin	10
Figure 4: Melting Curves	15
Figure 5: Melting Curves of Wild-type and Mutants	17
Figure 6: Chemical Structures of Osmolytes	18
Figure 7: Melting Curves of Select MBP-OLFs Proteins in Presence of Osmolytes	20
Figure 8: Characterization of MBP-OLF and Mutants by CD	30
Figure 9: Characterization of Cleaved MBP-OLF, SNPs, and Mutants by CD	30
Figure 10: Structure of Thioflavin T	31
Figure 11: Size-Exclusion Chromatography	35

LIST OF SYMBOLS AND ABBREVIATIONS

POAG	Primary Open-Angle Glaucoma
OLF	Olfactomedin
SNP	Single Nucleotide Polymorphism
TEM	Trabecular Meshwork
HTM	Human Trabecular Meshwork
ER	Endoplasmic Reticulum
MBP	Maltose Binding Protein
T_m	Melting Temperature
TMAO	Trimethylamine *N*-oxide
4-PBA	4-Phenylbutryate
CD	Circular Dichroism
ThT	Thioflavin T

SUMMARY

Myocilin, expressed in the trabecular meshwork cells of the human eye, has been linked to inherited primary open-angle glaucoma (POAG), an illness characterized by increased intraocular pressure and irreversible vision loss(*1*)(*1*)(*1*)(*1*)(*1*)(*1*)(*1*)(*1*)(*1*). Disease-causing point mutation variants of myocilin, over 90% of which are found in its olfactomedin (OLF) domain, cause its aggregation in the endoplasmic reticulum (ER) of trabecular meshwork cells, as shown by cellular secretion studies. This accumulation of protein triggers unfolded protein response within these cells, which ultimately leads to apoptosis. The cellular debris has been suggested to compromise the trabecular meshwork, lead to poor regulation of aqueous humor flow and increase in intraocular pressure, and finally, to an early glaucoma diagnosis. Since its discovery in 1997, biophysical characterization of myocilin has been hindered by poor expression and low yields. I overcame this severe limitation in the study of myocilin by fusing the full length and OLF domains independently to maltose binding protein (MBP) via a short linker. Using the MBP-OLF construct, I used site-directed mutagenesis to generate a total of 21 reported disease-causing variants, which were likewise expressed and purified.

The stability of wild-type and mutant OLFs were assessed in order to gain insight into the biophysical roles of particular mutations in glaucoma. I adapted differential scanning fluorimetry, a method to follow the unfolding of a protein using a fluorescence of a dye sensitive to hydrophobic regions of a protein that become exposed during denaturation, for facile stability measurements of OLFs without the removal of MBP. Initially, the melting temperatures for wild-type OLF and four variants (D380A, I477S, I477N and K423E) were determined, ranging in phenotype from mild to severe,

respectively. A correlation between the extent of glaucoma severity and thermal stability of the particular mutant was observed during these initial trials, and trends were solidified by the addition of the melting temperatures of 19 more other disease-causing variants.

Next, I investigated the possibility of restoring mutant OLF stability to wild type levels with small molecules. This experiment was motivated by a therapeutic approach for myocilin glaucoma that aims to restore mutant myocilin stability, and thus enable its secretion, via escaping detection by endoplasmic reticulum quality control proteins. The net effect of such a therapy would be to alleviate stress of the cell and keep the trabecular meshwork intact. As proof of principle for this therapeutic direction, changes in the stability of OLF mutants were measured in the presence of osmolytes, compounds known to stabilize proteins primarily by their effect on the protein backbone. Of the seven osmolytes tested, sarcosine and trimethylamine-*N*-oxide restored the melting temperature of the mutant OLF to approximately that of wild-type.

Taken together with previous qualitative assays examining the extent of solubility of mutant myocilins in Triton X-100, and temperature-sensitive secretion from mammalian cells, combined with trends observed in age of diagnosis of glaucoma, my work shows a strong correlation between the biophysical properties of the mutant and severity of glaucoma. Specifically, variants with low melting temperatures are associated with more severe glaucoma phenotypes, are generally insoluble in Triton X-100, and are neither secreted from cells at 37 °C nor at 30 °C. Conversely, three mutants (G246R, A427T, and A445V) have similar melting temperatures, and comparable circular dichroism spectra to wild-type, suggesting an error in their assignment as pathogenic. Lastly, three reported variants caused by single nucleotide polymorphisms (E352Q,

E396D, and K398R) displayed melting temperatures above wild-type OLF, confirming that these are also benign mutations.

Overall, my thesis describes a quantitative correlation between glaucoma phenotype and reported-disease causing mutations. This work offers a quantitative and facile evaluation method to distinguish disease-causing mutants from benign mutants for glaucoma. This approach is likely to be further applicable to other genetic diseases caused an assortment of missense mutations.

CHAPTER 1

PROTEIN EXPRESSIONAND PURIFCATION

Introduction

Glaucoma, the leading cause of blindness, currently affects about 70 million people worldwide (*2*) This illness is characterized by irreversible blindness and an increased intraocular pressure (*1*). The control of the flow of aqueous humor, found within anterior portion of the eye, is thought to contribute to the intraocular pressure. However, this regulation of flow in relation to glaucoma is poorly understood (*3*). Most individuals suffer from sporadic glaucoma but others inherit the disease, the most common inherited form being primary open-angle glaucoma (POAG). Through genetic-linkage studies performed in the past several years, three disease-causing genes have been correlated with POAG, the myocilin gene being the most common (*1*).

Myocilin (gi accession: 4557779, geneID 4653) is found in the trabecular meshwork (TEM) of the eye, among other places both inside and outside of the eye. As a secreted glycoprotein, myocilin is thought to contribute structurally to the TEM and minimize the movement of the human trabecular meshwork (HTM) cells (*3*, *4*). Myocilin has several distinct features: a signal sequence (Figure 1A, red), a linker with a proposed N-glycosylation site, a coiled-coil leucine zipper (Figure 1A, green), and an olfactomedin (OLF) domain (~30 kDa) (Figure 1A, yellow). The leucine zipper has been shown to interact with other known extracellular matrix proteins and has been proposed to be the site for dimerization (*5*-*7*). The OLF domain has been shown to be involved in adhesion and growth of neurons in mammalian brain development (*8*). No structure of either the OLF domain or myocilin reported. Therefore, studying myocilin cannot only give insight

into its role in glaucoma, through the study of disease-causing mutants, but also present information about the structure of the OLF domain.

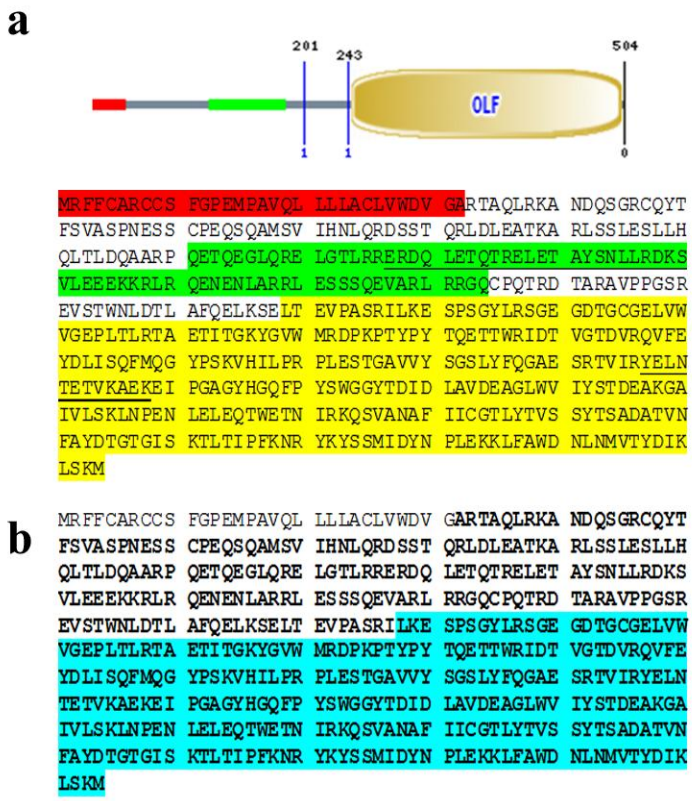

Figure 1. Myocilin domains and sequence. (A) Feature domains of myocilin (red, signal sequence; green, coil-coiled leucine zipper; yellow, OLF domain). Underlined segments—peptides identified by mass spectrometry. (B) Sequences of studied constructs (bold, full-length; blue, OLF)

Most of the reported disease-causing mutations occur within the OLF domain of myocilin, and the results from recent studies implied that these mutants take on a toxic gain-of-function mechanism (*3*). Mutant myocilin is retained in the endoplasmic reticulum (ER), instead of being secreted to the TEM like wild-type. Cellular studies have shown that at lowered temperatures, some mutants can be secreted, implying that toxic effects can be reduced with slower protein production allowing for proper folding

(*9-12*). Additionally, homozygous and heterozygous myocilin knockout mice along with individuals with an N-terminal truncated myocilin both display no ocular abnormalities (*13, 14*), implying that mutant myocilin is the source of toxicity within the HTM cells.

One hypothesis to overcoming the toxic effects of mutant myocilin may be achieved by increasing secretion of these mutants, thus reducing cellular stress caused by aggregation. To achieve this, mutant myocilin must pass the ER quality control machinery. Any protein folded in the ER, such as myocilin, is screened by ER quality control before being marked for secretion (*15*). If any irregularity is noticed, that protein is retained in the ER and either an attempt is made to refold it or it is marked for degradation. The cellular secretion studies at lowered temperature mentioned earlier imply that mutant myocilin probably has a slight thermal instability in the mutated domain but overall has a native three-dimensional structure. This slight instability can be detected by the ER quality control machinery that not only looks for exposed hydrophobic areas but also abnormalities due to biophysical properties (*15*). Retention of mutant myocilin in the ER that has not passed ER quality control leads to aggregation, which causes stress on the HTM cells and eventual apoptosis (*10, 12, 16-18*). The death of the HTM cells has been suggested to compromise the integrity of TEM, which can no longer regulate the aqueous humor. With the lack of regulation, the pressure increases, causing retina degradation, a key symptom of glaucoma. Therefore, glaucoma is not directly caused by mutations in myocilin but rather a collection of issues initiated by these mutations.

If mutant myocilin could pass ER quality control, it would be secreted as normal. Finding a mechanism to stabilize the native state of mutant protein is a therapeutic

avenue in general for protein-misfolding illnesses (*19*). Secreting the mutant protein from the ER is thought to decrease the toxicity along with the stress level of the cell (*20*) . After secretion, the cell would not be in danger of apoptosis. However, without knowledge of the structure, a top-down approach is needed to identify ligands or small molecules that could stabilize the folding of mutant protein.

In this thesis, the expression and purification of myocilin is described, resolving a previous limitation in the literature. This issue was solved by creating a fusion protein with maltose binding protein (MBP). A truncated myocilin, containing the OLF domain, and full-length myocilin were both expressed and purified (Figure 1B). In addition, 24 mutants (both disease-causing and benign) were also expressed and purified. An assay was developed to study the thermal stability of both the wild-type and mutant OLF constructs. General trends are presented based not only on the experimentally determined melting temperatures of the proteins but also with data from other published studies, including solubility, secretion and symptomatic information of afflicted individuals. Additionally, several small molecules were shown to increase the stability of both the wild-type and mutant myocilins, which could be used in future studies to create a screening method for ligands. Finally, additional biophysical characterization techniques are detailed, giving further insight into myocilin.

Expression and Purification of Wild-type MBP-OLF

Initially, a truncated myocilin composed of only the OLF domain was expressed first since 90% of reported disease-causing mutations are found in this region (*3*). Previous studies reported issues with expression and purification due to low yields and insolubility from *in vitro* expression (*7, 21-24*). Generally, concentrations between 0.05-

0.1 mg/mL were used in experiments and any higher concentration led to aggregation (*7*). Additionally, myocilin aggregates have been reported in cellular studies and in overexpression of wild-type myocilin in *D. melanogaster* eyes (*16, 18*). To overcome the issues of low yield and insolubility, a fusion protein was created with a N-terminal MBP, which has been shown in previous studies to assist in proper folding of recombinant proteins in *E. coli* (*25*). The protein yield was high (~2 mg/L) and the purity was homogeneous; thus, the protein was concentrated to ~10 mg/mL or higher. MBP and the OLF domain were connected by an eight amino acid linker, which was chosen over longer linkers to avoid elution with GroEL, an *E. coli* folding chaperone. This linker contains a Factor X_a cleavage site, a commercially available protease, to allow for separation of MBP and OLF. Expression trials were performed with various broths and different growth temperatures after induction and it was determined that Superior broth media and growth at 18°C overnight provided the best expression (*26*). Overall, the combination of these factors along with the use of a specialized *E. coli* strain contributed to an increased expression of MBP-OLF.

In the purification of wild-type MBP-OLF, a two column procedure was designed to isolate the monomeric fusion protein. First the wild-type MBP-OLF was purified by amylose-affinity chromatography, resulting in a mixture of MBP-OLF (aggregated and monomeric) and excess MBP, a result of cellular proteases. These fractions were then passed over a size-exclusion, or gel filtration, column to isolate monomeric MBP-OLF. The gel filtration purification yielded three distinct peaks (Figure 2B). The first peak corresponds to the material in the void volume, those proteins above the size cutoff to be efficiently separated by the gel filtration column and is composed of MBP-OLF

aggregates. The next peak is monomeric MBP-OLF (~72 kDa) and the final peak is excess MBP (~42 kDa) (Figure 2B) (*26*). Aggregation, as mentioned earlier, has been observed in cellular studies (*16, 27*) but the relationship between these two sets of aggregates is unclear. However, insight can be gathered from the predicted amyloid regions (*28*) and the high β-sheet content observed in the OLF domain (*21*).

To isolate monomeric OLF from MBP, cleavage of the monomeric MBP-OLF by Factor X_a was performed at 37 °C (*26*). Figure 2A shows purified wild-type MBP-OLF on the left (Lane 2) and purified cleaved OLF (~31 kDa) on the right (Lane 2), which was purified in the same manner as uncleaved after the cleavage reaction. Each gel has molecular mass standards in Lane 1 (Figure 2A).

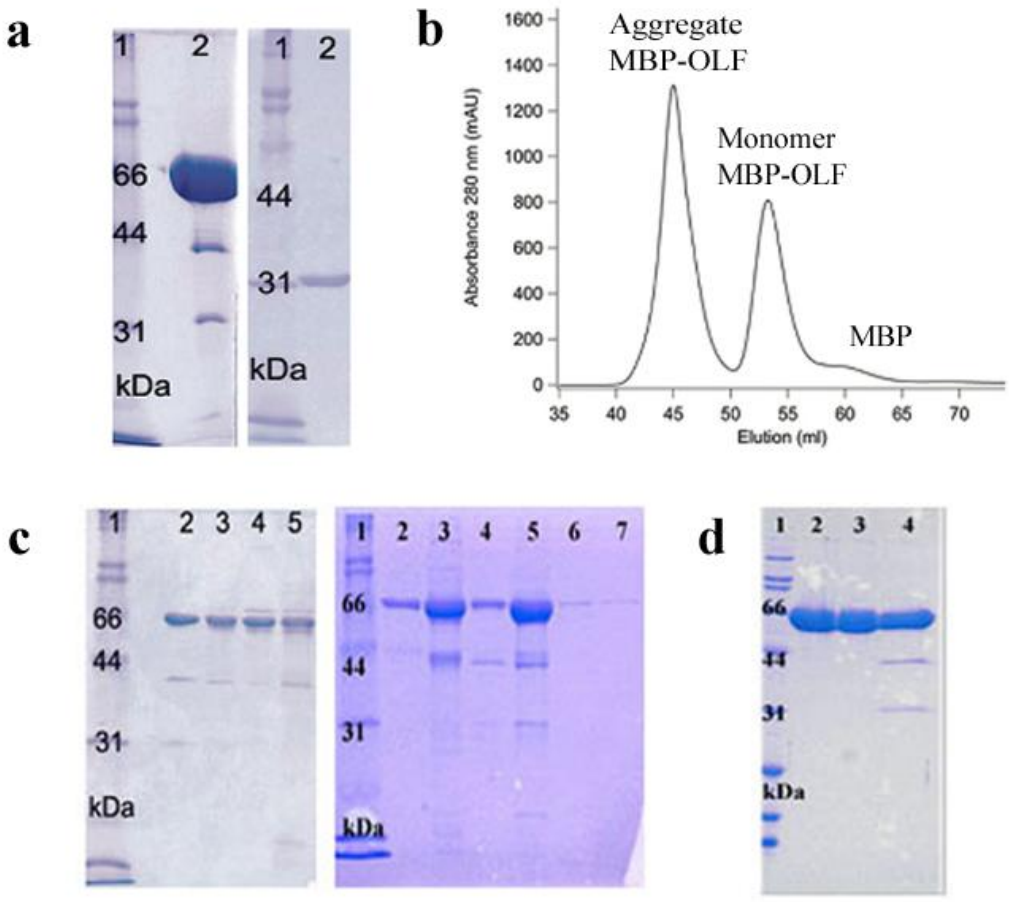

Figure 2. OLF Purification. (A) SDS-PAGE analysis of wild-type MBP-OLF (left) and cleaved OLF (right). (B) Sample gel-filtration chromatograph of wild-type MBP-OLF. (C) SDS-PAGE analysis of MBP-OLF mutants. (left gel) Lane 2—D380A; Lane 3—I477S; Lane 4—I477N; Lane 5—K423E. (right gel) Lane 2—wild-type; Lane 3—A427T; Lane 4—C433R; Lane 5—I499F; Lane 6—T377M; Lane 7—V426F. (D) SDS-PAGE analysis of MBP-SNPs. Lane 2—E352Q; Lane 3—E396D; Lane 4—K398R. Lane 1 for all gels has molecular mass standards.

Expression and Purification of Mutant MBP-OLFs

Initially, four mutants (D380A, I477S, I477N, and K423E) were chosen because they represented a varying severity of disease-causing mutations. D380A is considered a mild mutant, I477S is moderate and K423E and I477N are both severe. These classifications are based on age of onset and intraocular pressure of the affected individual (*12*). Twenty more mutants were added to the study in order to look for overall trends and make general conclusions about disease-causing mutations and their role in glaucoma (see Table 2 for full list of mutants).

The expression and purification of the mutant MBP-OLFs followed the same procedure described above for wild-type MBP-OLF. The gel filtration column gave the same three distinct peaks as wild-type OLF (*26*). However, depending on the mutant, the size of the aggregation peak varied (Figure 11B-C), implying various propensities of aggregation, discussed further in Chapter 3. Figure 2C shows SDS-PAGE analysis of purified mutant MBP-OLF. The left gel displays the initial four mutants (Lane 2—D380A, Lane 3—I477S, Lane 4—I477N, and Lane 5—K423E). On the right, the gel contains a selection of the twenty additional mutants (Lane 2—Wild-type, Lane 3—A427T, Lane 4—C433R, Lane 5—I499F, Lane 6—T377M, and Lane 7—V426F). Each gel has molecular mass standards in Lane 1 (Figure 2C).

In addition to disease-causing mutations, three mutants resulting from single-nucleotide polymorphisms (herein referred to as SNPs) were expressed and purified. SNPs are mutations that occur in more than one percent of the population, creating genetic variation (*29*). E352Q (rs61745146), E396D (rs61730975) and K398R

(rs56314834) were chosen from the Database of Single Nucleotide Polymorphisms for this study since they were the only missense mutations at the time of study (*30*). These SNPs were expressed and purified in the same manner as the disease-causing mutants and were selected to serve as a control, as they are considered benign mutations. They displayed similar peaks on the gel filtration chromatograph as wild-type and mutant MBP-OLF but the aggregation peak was smaller than the monomer peak, which was the opposite of the other chromatographs (Figure 11A). This difference suggests that these SNPs have a lower propensity for aggregation, which is discussed further in Chapter 3. Finally, Figure 2d shows SDS-PAGE analysis of the three SNPs (Lane 2—E352Q, Lane 3-E396D, and Lane 4—K398R). Lane 1 has the molecular mass standards (Figure 2D).

Three of the mutant MBP-OLFs (A427T, G246R, and A445V) along with the three SNPs were cleaved with Factor X_a. Their melting temperatures are close to or above wild-type MBP-OLF so the cleavage reaction at 37 °C is possible. The other mutants, as described in Chapter 2, have melting temperatures at about 37 °C and therefore, could not be cleaved in this manner. Further optimization with Factor X_a could allow for cleavage of the mutants but for this thesis, only these six mutants were cleaved for circular dichroism studies.

Expression and Purification of Full-Length Myocilin

With the truncated OLF domain, only part of myocilin can be studied, which is appropriate for the investigation of mutations and their role in glaucoma. However, for characterizing myocilin, a full-length protein would be needed. The full-length myocilin gene was first subcloned into the pET32 vector, which creates a gene encoding a Trx-Tag™ thiroedoxin fusion protein. This construct also has a His-tag, which allows for

nickel affinity chromatography. However, the yields were moderate, nothing compared to amylose affinity chromatography used with MBP-OLF. Therefore, the full-length gene was subcloned into the pMAL vector, creating a fusion protein with MBP. Figure 3B shows SDS-PAGE analysis of amylose-purified full MBP-myocilin (Lane 2). There are three prominent bands in Lane 2. One band around ~97 kDa corresponds to the fusion protein and another one at ~57 kDa is cleaved full myocilin, most likely by cellular proteases. The final band is about ~42 kDa, which represents excess MBP.

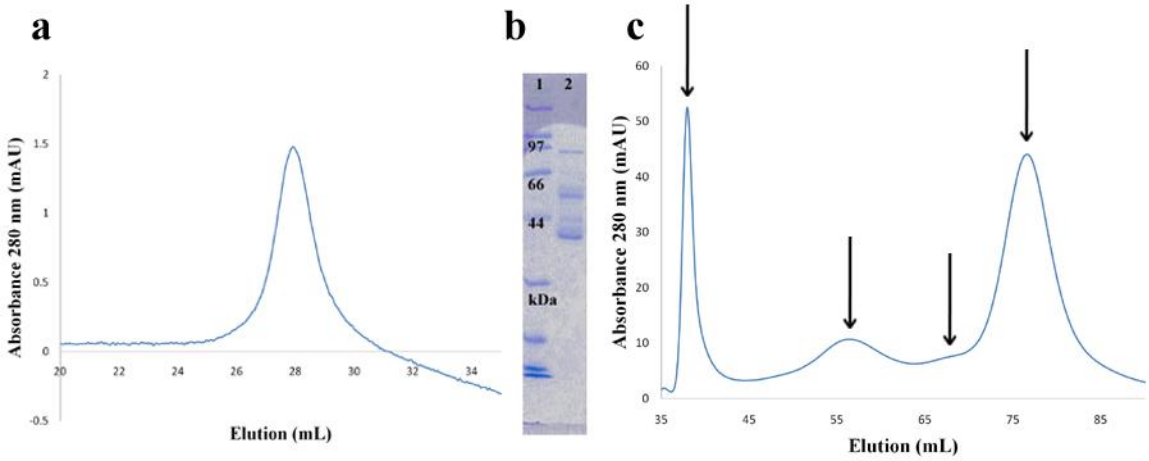

Figure 3. Purification of Full Length Myocilin. (A) Heparin chromatograph. (B) SDS-PAGE analysis of purified full MBP-myocilin. Three bands in Lane 2: Full MBP-myocilin (~96 kDa), cleaved Full (~57 kDa), and excess MBP (~42kDa). Lane 1 has molecular mass standards. (C) Sephacryl S-300 chromatograph (arrows indicate peaks).

This full length fusion protein was expressed in the same manner as wild-type MBP-OLF but different purification methods were applied after isolation of the protein from amylose affinity chromatography. First, the sample was passed over a heparin column, which was used as a purification method in previous studies (*7*). Heparin is a

sulfated polysaccharide that is a major anticoagulant and interacts with many proteins, mostly α-helical in nature. However, the nature of these interactions is not well understood (*31*). Myocilin may bind the heparin column through the coil-coiled leucine zipper, which is α-helical. The protein was eluted at ~35% Buffer B (10 mM Sodium Phosphate, 2 M NaCl, pH 7) shown in Figure 3A.

An additional chromatographic method used with full MBP-myocilin was a gel filtration column with a high molecular weight cutoff, Sephacryl S-300. Four distinct peaks eluded from the column (arrows, Figure 3C). The first is the void volume, which contains the aggregated full MBP-myocilin, while the second peak is monomeric full myocilin-OLF (~96 kDa). The third peak represents cleaved myocilin (~54 kDa), most likely resulting from proteases, and finally, the fourth peak is excess MBP (~42 kDa).

To confirm the identity of the purified protein, a trypsin digest was done on samples from the heparin and S-300 purifications. Trypsin is a serine protease that cleaves at a specific protein sequence (after an arginine or lysine residue). Trypsin digest is used to identify proteins because trypsin cleaves a protein into multiple smaller peptides that can be detected by mass spectrometry. The peptides are separated based on size by the mass spectrometer and their resulting masses are run through a database, which will identify the protein based on the peptides as the cleavage products (*32*). Table 1 lists the peptides generated from the heparin column sample. The underlined segments in Figure 1A are the sequences that were identified via trypsin digest, confirming that full-length myocilin was eluted from the heparin resin. The protein that eluded from the S-300 resin could not be identified, mostly due to a containment sample.

Table 1. Identified peptides via mass spectrometry from full-length myocilin.

Residue Range	Sequence	Calculated Mass (Da)	Observed Mass (Da)
148-156	DKSVLEEEK	1076.547	1076.5576
159-168	LRQENENLAR	1242.6549	1242.6864
169-179	RLESSSQEVAR	1261.6495	1261.6813
127-136	ERDQLETQTR	1275.6288	1275.6675
137-147	ELETAYSNLLR	1308.6794	1308.7184
347-358	YELNTETVKAEK	1424.7267	1424.7727

Expression and isolation of monomeric wild-type MBP-OLF and mutants allowed for characterization of these proteins. The thermal stability of each was determined, described in Chapter 2, and additional biophysical techniques were performed to gather further information about myocilin, discussed in Chapter 3. However, for full-length myocilin, the expression and purification is the only work included in this thesis. Now with established expression, further optimization with purification of full-length myocilin will allow for future research in the characterization of this protein.

CHAPTER 2

DEVELOPMENT OF A QUNTITATIVE ASSAY

A novel thermal stability assay was developed to compare wild-type and mutant MBP-OLF. This assay was adapted from a previously published fluorescence assay, designed to study the stability of proteins in the presence of buffers, salts and other small molecules (*33*). In this experiment, a real-time (RT)-PCR was used since it can detect the emission of SYPRO orange, a dye known to bind to the hydrophobic portion of a protein. As the protein unfolds due to the increase in heat, the signal of SYPRO orange also increases due to the binding onto exposed hydrophobic areas of the protein (*33*). The melting temperature (T_m), the point at which half of the protein is folded and half is unfolded, can be determined from the melting curve. It is the midpoint of the curve, assuming a two-state transition. The higher the T_m, the more stable the protein. Trends can be deduced from the melting temperatures of the protein alone and in the presence of osmolytes.

Since MBP-OLF is a fusion protein, control experiments were performed to determine if the melting curves of OLF-MBP could be distinguished from one another. First, the melting temperature of MBP was studied with and without maltose. Previous studies have shown that the binding of a ligand increases the stability of a protein (*34*); the binding of maltose, the ligand for MBP, should raise the T_m of MBP to be higher than OLF's. The melting temperature of MBP without maltose was 56.1 °C but in the presence of maltose the T_m shifted to 67.1 °C (Figure 4A) (*26*). The melting temperature was increased by 11 °C, significant enough to separate from the melting of OLF. However, maltose could affect the melting of OLF. Figure 4B shows the melting curves

of cleaved OLF with and without maltose and MBP-OLF with maltose. The three curves overlay exactly showing that maltose has no effect on the melting temperature of OLF. Finally, MBP-OLF's melting temperature was determined with and without maltose. Without maltose, the T_m of the fusion protein was 51.8 °C but with maltose, two discernable transitions are seen (Figure 4C). The melting temperature of the first peak is 52.7 °C and the second is ~67 °C. The first curve is shown trimmed in Figure 4B, which overlays with the melting curves of cleaved OLF, indicating that the first transition is the melt of OLF. The second temperature of 67 °C is close to the melting temperature of MBP in the presence of maltose (67.1 °C). The second transition can be concluded to be the melting of MBP. Overall, the melting of OLF can be distinguished from the melting of MBP by adding maltose.

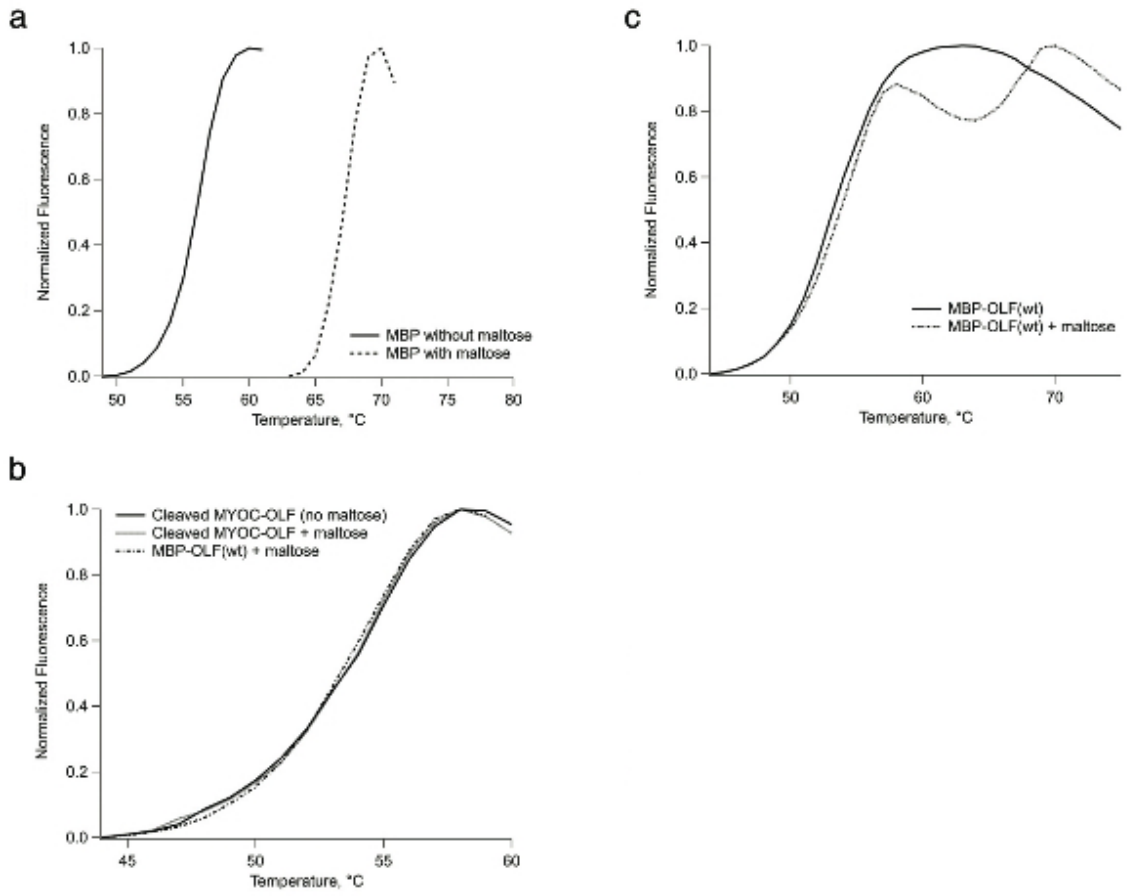

Figure 4. Melting Curves. (A) Cleaved OLF with and without maltose. (B) Cleaved OLF with and without maltose. (C) OLF with and without maltose.

After the T_m of wild-type MBP-OLF was determined, the T_m of the 21 disease-causing mutants and three SNPs were determined. Figure 5 shows the melting curves for all 24 proteins, grouped together with different colors. The mutants (K423E, I477N, and Y437H) with the lowest melting temperature are shown in red. C433R and I499F, in black, are group together due to their broad melting curve. Next the mutants with a medium melting temperature are split into blue (lower melting temperature) and light-blue (higher melting temperature). With the inclusion of wild-type in grey, the green melting curves describe the mutant proteins (A427T, G246R, G326R, and A445V) with the highest melting temperatures. Finally, the SNPs (K398R, E396D, and E352Q) are also colored in gray and show a T_m higher than wild-type MBP-OLF. Almost all of the mutants and wild-type show a sharp sigmoidal transition, indicative of a two-state unfolding. However, C433R and I499F have broad transitions, implying unfolding through a mechanism other than two-state.

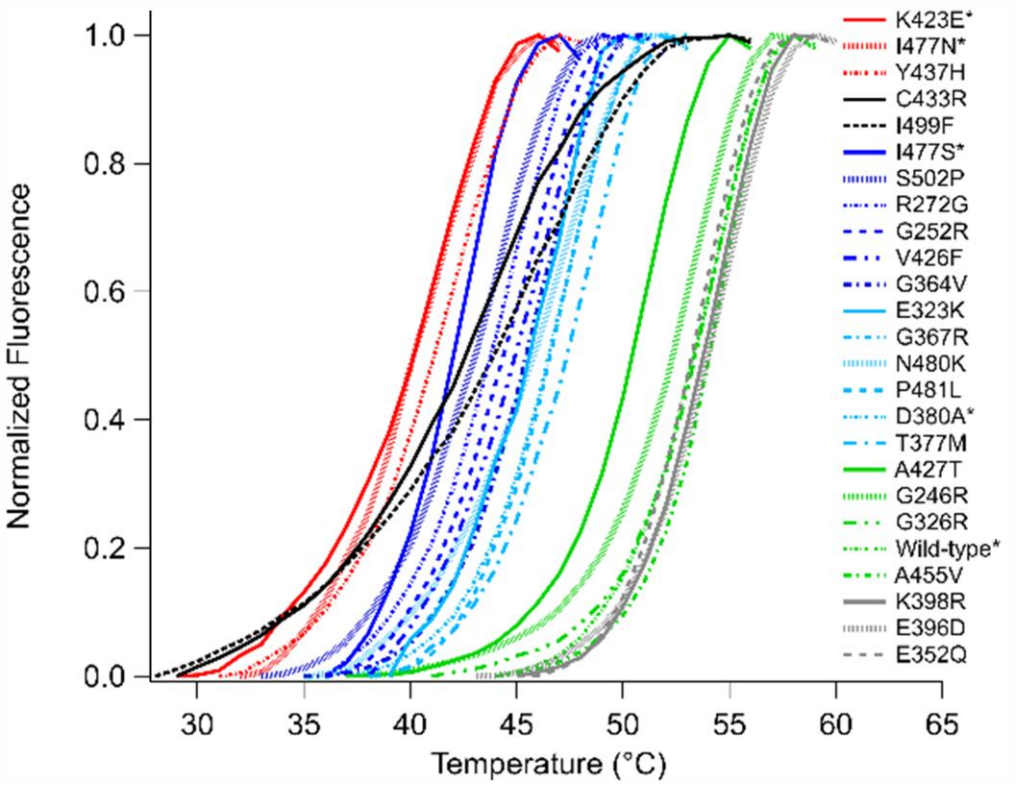

Figure 5. Melting Curves of Wild-type and Mutants.

The diseasing-causing mutants are generally less stable than wild-type MBP-OLF, signified by their lower melting temperatures. However, four mutants (A427T, G246R, G326R, and A445V) have T_m's near or above that of wild-type, suggesting that these mutations might not be disease-causing mutants or if they are, very mild disease-causing mutants. Additionally, the SNPs have melting temperatures above wild-type and are known to be benign mutations. Therefore, these four mutants are likely benign mutations instead of disease-causing mutations due to their high melting-temperature.

If the stability could be increased enough to pass ER quality control, then the mutant protein could be secreted into the trabecular meshwork, maintaining its integrity. A small molecule binding to or affecting the folding of mutant myocilin would be ideal to achieve this goal, especially for therapeutic use. In general, these molecules are known as

chemical, or pharmacological, chaperones when they are targeted for specific binding. Pharmacological chaperones have been studied numerous times for therapeutic use to increase thermodynamic stability of proteins (*19*, *35-38*). Drawing from these examples, wild-type and mutant myocilins were tested with seven common osmolytes, a subset of chemical chaperones, as a proof-of-concept that these mutants could be stabilized. These osmolytes are small molecules that maintain protein homeostasis in eukaryotic cells exposed to osmotic stress (*39*). Osmolytes destabilize the unfolded state of the protein, pushing the equilibrium towards the folded state by creating an environment unsuitable for the protein backbone (*40-43*). This shift in equilibrium towards the folded state stabilizes the protein.

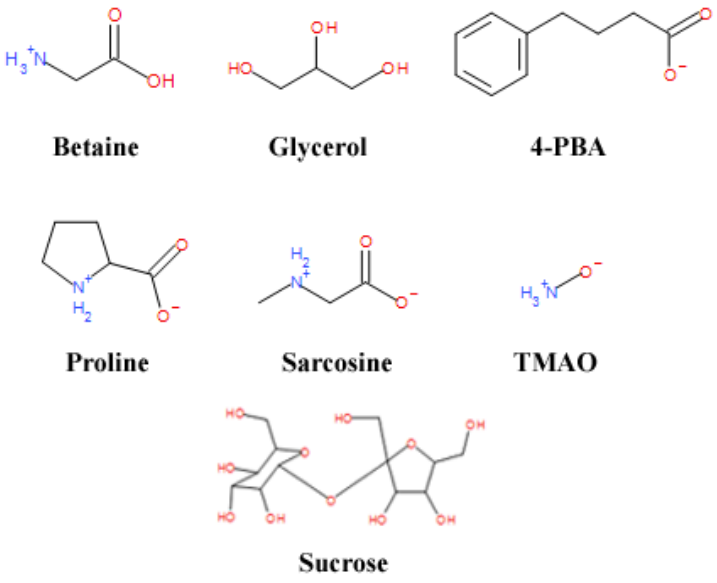

Figure 6. Chemical Structures of Osmolytes.

First, the effects of betaine, glycerol, proline, sarcosine, sucrose, trimethylamine *N*-oxide (TMAO), and 4-phenylbutyrate (4-PBA) (structures shown in Figure 6) were tested on cleaved OLF and MBP-OLF. The wild-type protein was examined first. If the wild-type mutant is stabilized by these osmolytes then the mutants should be as well. To determine if the effect of the osmolytes on the OLF domain of the fusion protein could be discerned, both cleaved OLF and MBP-OLF were tested. Figure 7A shows the melting curves of MBP-OLF protein in buffer along with the melting curves in the presence of osmolytes. All of the osmolytes, except 4-PBA, increased the melting temperature in the following order: sacrosine, TMAO, sucrose (~8-10 °C), proline, betaine, glycerol (~2-4 °C) (Figure 7A, Table 2) (*26*). The difference between the melting temperature of cleaved OLF and MBP-OLF was approximately 0.3 °C so the effect on the OLF domain could be distinguished. Therefore, only the melting temperatures for MBP-OLF are reported. Since 4-PBA had no effect on MBP-OLF, its melting curve is not displayed in Figure 7A but the melting temperature is reported in Table 2; this is the case for the mutants also.

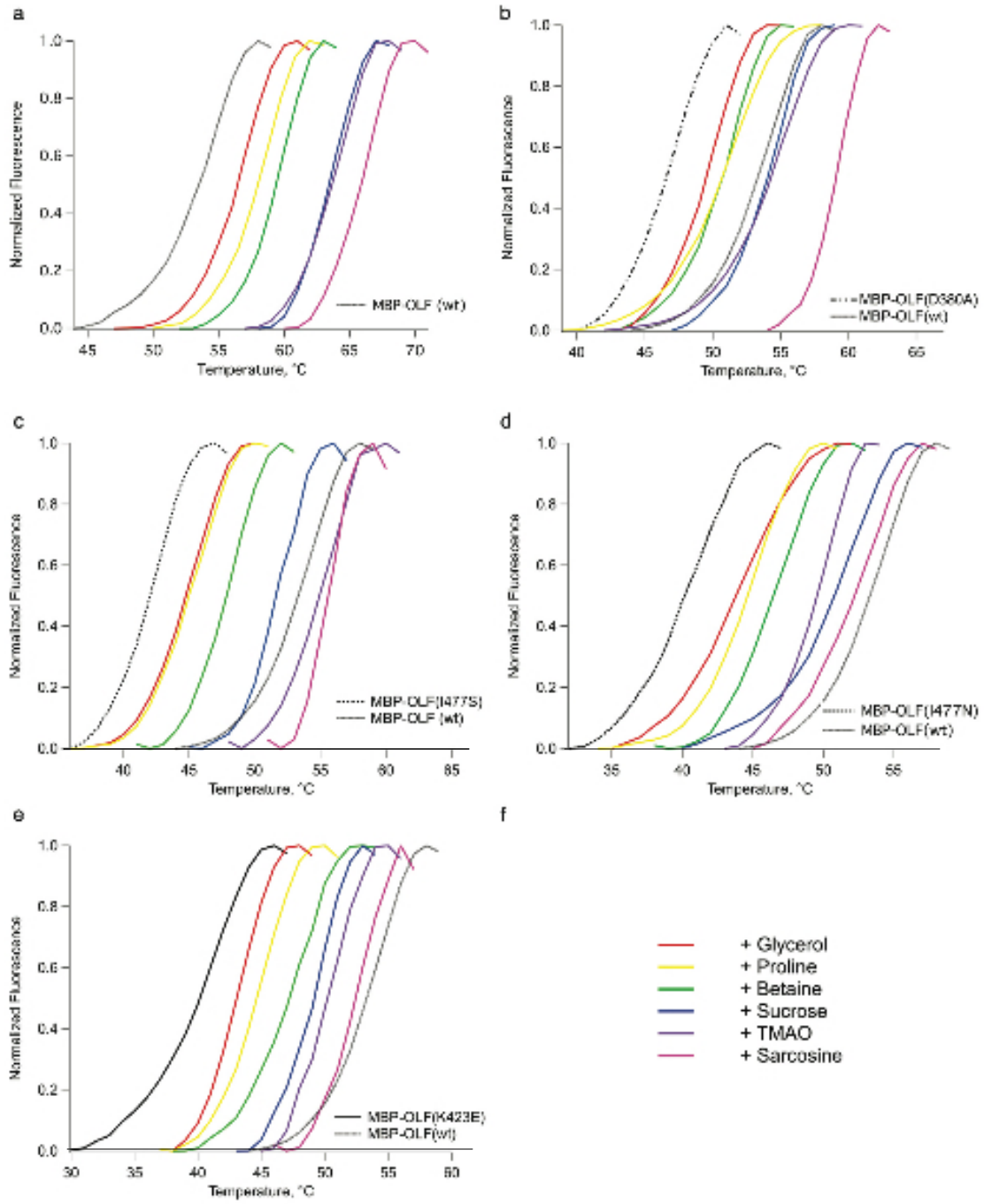

Figure 7. Melting curves of select MBP-OLF proteins in presence of osmolytes. (A) Wild-type MBP-OLF (B) D380A-MBP (C) I477S-MBP (D) I477N-MBP (E) K423E-MBP (F) Color key for osmolytes.

Figure 7 shows the melting curves of the initial four disease-causing mutants. Out of the seven osmolytes, sarcosine and TMAO had the greatest effect on these mutants, bringing the melting temperature close to or above the T_m of wild-type MBP-OLF in buffer. This trend continues for all of the remaining disease-causing mutants and three SNPs with an increase of T_m of seven degrees or higher for both sarcosine and TMAO (Table 2). Furthermore, Table 2 reports all of the melting temperatures in the presence of each osmolyte for all disease-causing mutants and SNPs, except for E323K and V426F. The melting temperatures of these two mutants in buffer and in TMAO were the only T_m's reported because the yield of MBP-OLF monomer from these mutants was very low. In addition to sarcosine and TMAO, sucrose increased the melting temperature but is not as effective for all mutants.

Table 2. Effect of osmolytes on T_m of OLF and mutants. ND = not determined.

Protein	Protein Only	Betaine	ΔT_m	Glycerol	ΔT_m	4-PBA	ΔT_m	Proline	ΔT_m	Sarcosine	ΔT_m	Sucrose	ΔT_m	TMAO	ΔT_m
Wild-type	52.7 ± 0.8	59.6 ± 0.8	6.9	56.0 ± 1.2	3.3	55.5 ± 0.5	2.8	57.2 ± 0.3	4.5	65.2 ± 0.6	12.5	64.3 ± 0.1	10.6	64.1 ± 0.7	11.4
D380A	46.7 ± 0.5	50.8 ± 0.2	4.1	49.5 ± 0.2	2.8	47.2 ± 0.1	0.5	49.9 ± 0.2	3.2	58.3 ± 0.6	11.6	54.2 ± 0.7	7.5	55.6 ± 0.9	8.9
I477S	41.9 ± 0.5	48.0 ± 0.6	6.1	45.1 ± 0.2	3.1	42.6 ± 0.1	0.7	45.3 ± 0.3	3.4	54.0 ± 0.4	12	50.7 ± 0.2	8.7	52.7 ± 0.8	10.7
I477N	40.1 ± 0.8	45.1 ± 0.7	4.9	43.7 ± 0.4	3.5	41.4 ± 0.4	1.3	43.8 ± 0.9	3.7	52.5 ±0.3	12.4	50.3 ± 0.9	10.2	50.1 ± 0.8	9.9
K423E	40.5 ± 0.1	45.9 ± 0.6	5.4	42.6 ± 0.2	2	38.9 ± 0.4	-1.6	42.7 ± 0.7	2.1	48.6 ± 0.6	8.1	46.3 ± 0.5	5.7	48.8 ± 0.7	8.3
MBP	67.1 ± 0.3	71.3 ± 0.6	4.2	68.2 ± 0.4	1.1	66.2 ± 0.1	-0.9	69.8 ± 0.6	2.7	75.1 ± 1.0	8	72.6 ± 0.8	5.5	74.4 ± 0.1	7.3
T377M	47.7 ± 0.2	53.5 ± 0.9	5.8	49.6 ± 0.4	1.9	47.1 ± 0.3	-0.6	51.3 ± 0.4	3.6	57.5 ± 0.6	9.8	53.6 ± 0.4	5.9	60.6 ± 0.7	12.9
A427T	50.5 ± 0.2	55.2 ± 0.7	5	52.7 ± 0.2	2.2	50.3 ± 0.3	-0.2	53.4 ± 0.4	2.9	59.3 ± 0.9	8.8	61.1 ± 0.6	10.6	61.1 ± 0.4	10.6
C433R	42.6 ± 0.4	47.3 ± 0.4	4.7	44.8 ± 0.3	2.2	40.8 ± 0.3	-1.8	45.7 ± 0.5	3.1	50.2 ± 0.5	7.6	44.1 ± 1.0	1.5	52.2 ± 0.6	9.6
I499F	44.4 ± 0.3	47.9 ± 1.0	3.5	46.3 ± 0.7	1.9	43.9 ± 0.3	-0.5	47.2 ± 0.8	2.8	55.9 ± 0.8	11.5	55.5 ± 0.7	11.1	56.3 ± 0.3	11.9
Y437H	41.4 ± 0.1	46.9 ± 0.9	5.5	44.0 ± 0.3	2.6	40.8 ± 0.2	-1.8	44.5 ± 0.3	3.5	48.1 ± 0.7	6.7	49.3 ± 0.5	7.9	50.4 ± 1.1	9
P481L	46.6 ± 0.1	51.0 ± 0.5	4.4	49.5 ± 0.4	2.9	46.2 ± 0.3	-0.4	48.8 ± 0.3	2.2	55.4 ± 0.1	8.8	55.1 ± 0.4	8.5	53.0 ± 0.8	6.4
R272G	44.7 ± 0.2	49.1 ± 0.4	4.4	48.0 ± 0.4	3.3	44.5 ± 0.5	-0.2	48.4 ± 0.2	3.7	52.5 ± 0.2	7.8	52.0 ± 0.8	7.3	51.7 ± 0.6	7
N480K	46.1 ± 0.3	50.0 ± 0.3	3.9	48.3 ± 0.2	2.2	45.7 ± 0.2	-0.4	47.8 ± 0.2	1.7	53.2 ± 0.4	7.1	52.5 ± 0.3	6.4	52.2 ± 0.8	6.1
N480L	46.3 ± 0.2	50.4 ± 0.3	4.1	49.2 ± 0.1	2.9	46.7 ± 0.4	0.4	48.1 ± 0.1	1.8	55.7 ± 0.7	9.4	57.4 ± 0.2	11.1	53.9 ± 0.6	7.6
S502P	43.0 ± 0.1	48.4 ± 0.4	5.4	46.2 ± 0.2	3.2	42.5 ± 0.1	-0.5	46.0 ± 0.2	3	53.3 ± 0.6	10.3	53.4 ± 0.3	10.4	52.9 ± 0.2	9.9
G364V	45.5 ± 0.2	52.8 ± 0.4	7.3	48.7 ± 0.1	3.2	45.8 ± 0.5	0.3	48.5 ± 0.2	3	55.8 ± 0.8	10.3	58.0 ± 0.3	12.5	56.7 ± 0.2	11.2
G367R	45.7 ± 0.1	51.4 ± 0.4	5.7	48.6 ± 0.1	2.9	45.4 ± 0.4	-0.3	48.4 ± 0.3	2.7	55.5 ± 0.8	9.8	57.9 ± 0.5	12.2	56.3 ± 0.3	10.6
A445V	54.2 ± 0.2	60.2 ± 0.4	6	56.8 ± 0.2	2.6	54.4 ± 0.3	0.2	56.4 ± 0.3	2.2	64.6 ± 0.2	10.4	66.2 ± 0.3	12	63.2 ± 0.6	9
E323K	45.6 ± 0.4	ND	-	ND	-	ND	-	ND	-	ND	-	ND	-	57.5 ± 0.5	11.9
V426F	45.1 ± 0.4	ND	-	ND	-	ND	-	ND	-	ND	-	ND	-	56.1 ± 0.8	11
G252R	44.8 ± 0.7	52.9 ± 0.8	8.1	48.7 ± 0.1	3.9	45.1 ± 1.0	0.3	48.3 ± 0.1	3.5	54.8 ± 0.9	10	57.0 ± 0.6	12.2	55.6 ± 0.8	10.8
G246R	52.7 ± 0.5	56.8 ± 0.3	4.1	55.3 ± 0.2	2.6	53.0 ± 0.5	0.2	54.5 ± 0.2	1.8	59.4 ± 0.4	6.7	62.5 ± 0.5	9.8	60.8 ± 0.7	8.1
G326R	52.9 ± 0.4	56.1 ± 0.5	3.2	55.3 ± 0.3	2.4	52.8 ± 0.2	-0.1	54.7 ± 0.2	1.8	60.7 ± 0.4	7.8	62.6 ± 0.5	9.7	60.3 ± 0.4	7.4
K398R	53.8 ± 0.2	59.2 ± 0.2	5.4	56.2 ± 0.3	2.4	55.6 ± 0.1	1.8	53.8 ± 0.3	0	62.6 ± 0.6	8.8	64.7 ± 0.4	10.9	65.0 ± 0.6	11.2
E396D	54.1 ± 0.1	58.9 ± 0.2	4.8	56.3 ± 0.2	2.2	55.7 ± 0.3	1.6	54.1 ± 0.3	0	63.4 ± 0.2	9.3	67.5 ± 0.6	13.4	65.4 ± 1.0	11.3
E352Q	54.9 ± 0.5	59.1 ± 0.3	4.2	56.2 ± 0.2	1.3	53.4 ± 0.7	-1.5	53.9 ± 0.2	-1	64.5 ± 0.5	9.6	64.5 ± 0.2	9.6	64.0 ± 0.7	9.1

Combining previously published data and the melting temperatures reported, the mutants can be sorted and conclusions can be made based on this order as to their role in glaucoma. Table 3 shows the 20 disease-causing mutants, three SNPs and wild-type MBP-OLF ranked by the melting temperature in buffer only. Based on these melting temperatures and those in the presence of TMAO, the mutants can be categorized into four groups. Group 1 includes P380L and W286R with no melting temperature reported due to low monomeric yield because of a high propensity for aggregation. Next, Group 2 represents the mutants with the lowest melting temperature (I477N, K423E, and Y437H). Furthermore, these mutants were not stabilized by TMAO to wild-type's T_m unlike Group 3. Group 3 includes the mutants with mid-range T_m's, representing the largest group. Finally, the Group 4 includes the three SNPs and three disease-causing mutants (A427T, G246R, and A445V) with temperatures around the T_m of wild-type or higher.

Table 3. Compilation of data on myocilin glaucoma variants from this and previous studies. Variants are listed in order of T_m. NA= not available; -- = not applicable; TMAO = trimethylamine *N*-oxide; I = insoluble; PI = partially insoluble; S = soluble; N = No secretion; +/- = little secretion; +, ++, +++ = increasing amounts of secretion as defined by Gobeil et al.; pop. = population study, no age of diagnosis provided; fam. = familial study, no age of diagnosis provided. [a] Accession numbers for Database of Single Nucleotide polymorphisms (dbSNP, Build ID 131). Bethesda (MD): National Center for Biotechnology Information, National Library of Medicine. Available from: http://www.ncbi.nlm.nih.gov/SNP. [b] Shimizu and/or Zhou. [c] Gobeil and/or Liu. [d] References refer to are listed according to age of diagnosis.

Group	Mutation			T_m			Solubility Assay[b]	Secretion Assay[c]		Age(s) of Diagnosis	References[d]
				Protein only	+3M TMAO	ΔT_m		37 °C	30 °C		
1	P	370	L	NA	NA	NA	I	N	+/-	12, 12, 10.5	Shimizu, Rosza, Adam
	W	286	R	NA	NA	NA	NA	N	N	NA (pop.)	Fingert
2	I	477	N	40.1±0.8	50.1±0.8	9.9	I	N	+/-	26, 18, 18, Pop.	Shimizu, Rosza, Richards, Fingert
	K	423	E	40.5±0.1	48.8±0.7	8.3	I	N	N	19, 33, 30	Morisette, Bruttini, Faucher
	Y	437	H	41.4±0.1	50.4±1.1	9.0	I	N	+/-	NA (pop., fam.)	Fingert, Alward
3	I	477	S	41.9±0.5	52.7±0.8	10.7	I	N	+++	33	Adam
	C	433	R	42.6±0.4	52.2±0.6	9.6	I	N	N	15, 38	Vasconcellos
	S	502	P	43.0±0.1	52.9±0.2	9.9	I	N	N	19	Stoilova
	I	499	F	44.4±0.3	56.3±0.3	11.9	PI	+/-	+++	28, 29, 31	Shimizu, Brezin, Adam
	R	272	G	44.7±0.2	51.7±0.6	7.0	NA	N	++	33	Shimizu
	G	252	R	44.8±0.7	55.6±0.8	10.8	I	N	+++	26, 26	Shimizu, Rosza
	V	426	F	45.1±0.4	56.1±0.8	11	I	+/-	+++	21, 26	Shimizu, Rosza
	G	364	V	45.5±0.2	56.7±0.2	11.2	PI	+	+++	NA (pop., fam.)	Fingert, Alward
	E	323	K	45.6±0.4	57.5±0.5	11.9	I	+/-	+++	19, 19	Shimizu, Rosza
	G	367	R	45.7±0.1	56.3±0.3	10.6	I	N	+++	32, 34	Kanagavalli, Faucher
	N	480	K	46.1±0.3	52.2±0.8	6.1	I	+/-	++	32.3, 30-35	Adam, Hulsman
	P	481	L	46.6±0.1	53.0±0.8	6.4	I	N	++	33, NA (pop.)	Faucher, Fingert
	D	380	A	46.7±0.5	55.6±0.9	8.9	PI	+/-	+++	21	Stoilova
	T	377	M	47.7±0.2	60.6±0.7	12.9	PI	+	+++	38, 52, 40, NA (pop.)	Shimizu, Kanagavelli, Mackey, Fingert
4	A	427	T	50.5±0.2	61.1±0.4	10.6	S	+++	NA	73	Faucher
	G	246	R	52.7±0.5	60.8±0.7	8.1	I	N	++	20	Adam
	Wild-type			52.7±0.8	64.1±0.7	11.4	S	+++	NA	--	--
	K	398	R	53.8±0.2	65.7±1.3	11.9	S	NA	NA	rs56314834[a]	Fingert, Alward, Shimizu, Faucher, Melki, Hulsman
	E	396	D	53.1±0.1	65.4±1.0	12.3	NA	NA	NA	rs61730975[a]	NA
	A	455	V	54.2±0.2	63.2±0.6	9	S	+++	NA	63, NA (pop.)	Faucher, Fingert
	E	352	Q	54.9±0.5	63.9±0.7	9.0	NA	NA	NA	rs61745146[a]	NA

Three other sources of data were included in Table 3 from which inferences can be made when combined with the melting temperatures. The results from a solubility assay are reported for most mutants; in Table 3, NA stands for not applicable for those mutants not included in these experiments. In this assay, the solubility of each protein in the presence of a detergent, Triton-X 100, was investigated. Those proteins found in the soluble portion were deemed as benign mutations while any mutant in the insoluble fraction was considered disease-causing (*44*, *45*). In Table 3, I represents insoluble, PI means partially insoluble, and S stands for soluble in the "Solubility Assay" column. Referring back to the four groups above, the proteins of Groups 1 and 2 are completely insoluble while Group 3 proteins are a mix of insoluble and partially insoluble. In Group 4, all proteins are soluble except for one, G246R (Table 3). Generally, most of the proteins are insoluble, which according to the guidelines set forth by Zhou *et al*, makes all of these disease-causing mutants. However, Group 4 would be considered benign mutations since most of them are soluble, suggesting that the reported disease-causing mutants in this group might have been mislabeled or just very mild mutants.

The secretion of each mutant from cells at two different temperatures is shown in Table 3. These cells were grown initially at 37 °C and the amount of protein secreted was determined qualitatively through immunobloting. Some of the mutants showed secretion at 37 °C but the temperature was lowered to 30 °C to see if the other mutants might be secreted (*9, 12*). In Table 3, in the "Secretion Assay" column, N stands for no secretion, +/- means little secretion and +, ++, and +++ represents increasing secretion, according to Gobeil *et al* (*9*). Groups 1 and 2 proteins show no secretion at 37 °C and partial secretion at 30 °C. Proteins in Group 3 are a mixture of no secretion and little at 37 °C but at 30 °C

almost all of the mutants are secreted. Finally, proteins in Group 4 are secreted at 37 °C, rendering the experiment at 30 °C unnecessary. Similar to the trend of the solubility assay, the first three groups have little secretion at 37 °C while the fourth group has normal secretion, providing more evidence for these mutations being benign. However, at 30 °C, there is a trend among the first three groups. Groups 1 and 2 did not secrete or had little secretion even at 30 °C, implying that the mutations are very unstable. Conversely, Group 3 had secretion at 30 °C, showing that the mutants are only moderately unstable. The lower temperature is further away from the T_m so the probability of the protein being folded is higher. Also at the lower temperature, the mechanisms in the cell are slower so the protein has a better chance of folding correctly.

Finally, the age of diagnosis of glaucoma is reported for each mutant in Table 3 when available. These data were collected through genetic studies looking at either families or populations for individuals with glaucoma. Once an individual was identified, their myocilin gene was sequence and if any mutation was found, it was reported as a disease-causing mutation. Mutations identified in families and populations often overlapped and were published in multiple studies (*46-60*). A correlation was expected to arise between the age of diagnosis and the order of the severity of the mutants. However, although each study uses similar methods of diagnosis, no clear guidelines were established when defining age of diagnosis. Since the ages reported are only for diagnosis, the actually age of onset is unknown and therefore, a correlation cannot be made between the ranking of severity of the mutants and the reported ages.

However, conclusions can be made if all of the data presented in Table 3 is analyzed together. Mutants in Groups 1 and 2 were insoluble and had not or hardly

secreted; therefore, they can be considered severe mutations. Generally, the individuals with these mutations are younger when they are diagnosed with glaucoma (Table 3). Proteins in Group 3 were insoluble to partially insoluble and efficiently secreted at 30 °C, suggesting that they are moderate mutations. Here the age of diagnosis data is varied greatly, so no correlation can be made but the mutants can still be considered moderate based on the other data. Finally, the mutants in Group 4 could have easily been mislabeled as disease-causing mutations. Those individuals with the A427T or A445V mutation, who were aged 63 and 73 at diagnosis respectively (Table 3), could have developed glaucoma from another source than these mutations (*50*). Therefore, these mutations could be considered benign or very mild mutations, further supported by the results from the solubility assay and secretion studies.

CHAPTER 3

BIOPHYSICAL CHARACTERIZATION

In studying the structure of wild-type myocilin, circular dichroism (CD) was used to discern information about its secondary structure in comparison to the mutant myocilins. Additionally, thioflavin T, a fluorescent dye, was used to determine the nature of the aggregates observed during gel-filtration purification. Using these biophysical techniques and comparing the propensity for aggregation of wild-type and mutants, new insight on myocilin's structure could be inferred and possibly offer implications for its role in glaucoma.

Circular Dichroism

Circular dichroism is a technique used in biochemistry to study the secondary structure of proteins. Circularly polarized light travels through a sample interacting with any chiral molecules. A spectrum is produced from these interactions and certain spectral fingerprints are used to assign secondary structure to the protein (*61*). For example, an α-helix has negative minima at 208 and 222 nm and a positive maximum at 190 nm, while a β-sheet has a minimum at 215 nm and a maximum at 198 nm (*62*). Figure 8 shows the CD spectra of wild-type MBP-OLF along with four mutants (D380A, I477N, I477S, and K423E) (*26*). In each spectrum, minima are observed at 208 and 222 nm, representing α-helical content. These minima come from MBP, which is primarily α-helical. Another minimum is observed around 217 nm, which is characteristic of a β-sheet. Myocilin is comprised of β-sheets however the α-helical signal from MBP overwhelms most of the signal from β-sheets, making it difficult to distinguish the contribution of myocilin to the CD spectrum. In contrast to the spectra of uncleaved MBP-OLF proteins, Figure 9 shows

the spectra of cleaved proteins. In these spectra, the minima at 208 and 222 nm are not observed and the β-sheet characteristic of myocilin is very prominent with the minimum at 217 nm. Also the spectra for the SNPs (E352Q, E396D, and K398R) overlay with wild-type OLF along with those of the mutants (A427T, G246R, and A445V). This overlap provides more evidence that there are no gross structural differences between the wild-type and mutant OLFs.

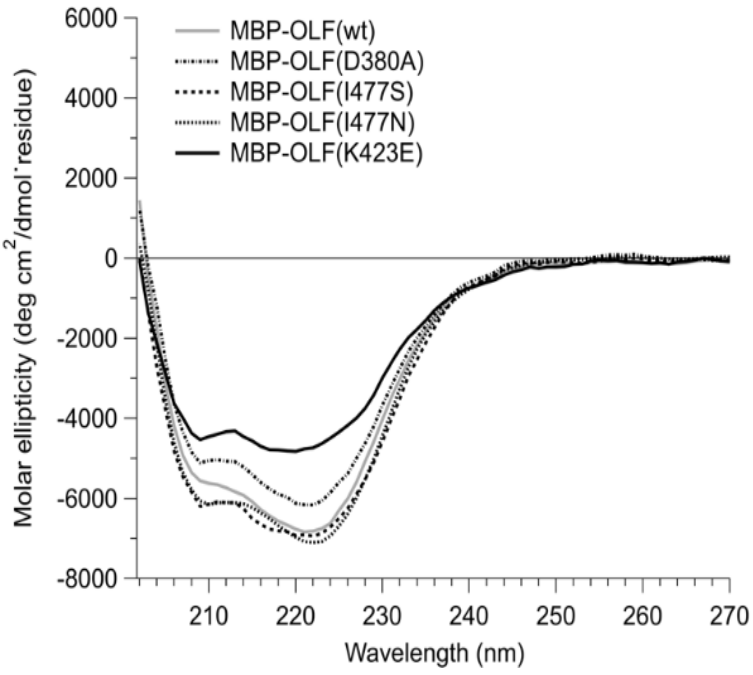

Figure 8. Characterization of MBP-OLF and mutants by CD.

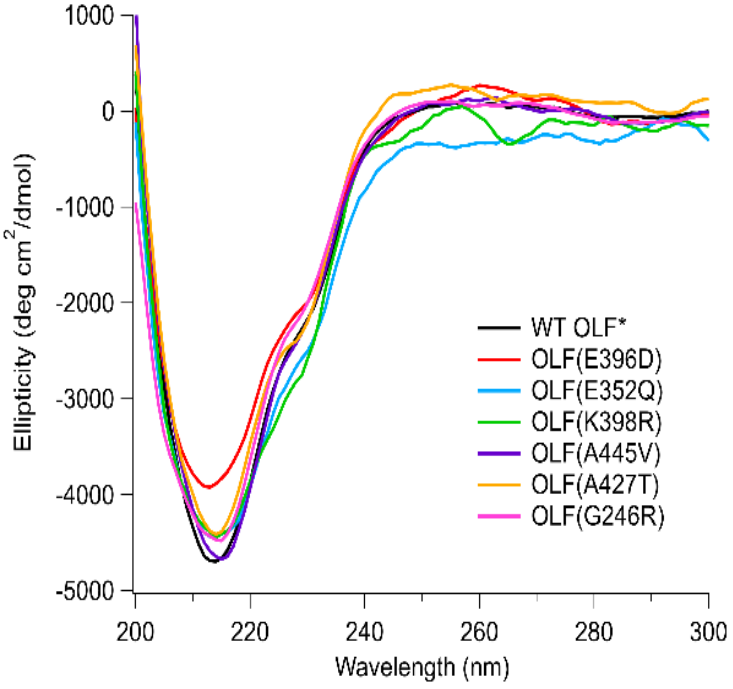

Figure 9. Characterization of cleaved OLF, SNPs, and mutants by CD.

Thioflavin T Assay

As mentioned previously, during gel filtration purification, aggregates of myocilin are observed in the void volume. One form that these aggregates can take is amyloid fibrils. One way to characterize a protein as a fibril is with the use of the fluorescent dye Thioflavin T (Figure 10). The fluorescence of thioflavin T (ThT) increases upon binding to amyloid fibrils. In the structure of ThT, the dimethylamino group on the right side of the molecule is hydrophobic while the benzothiazole group on the left is hydrophilic. This arrangement of hydrophilic and hydrophobic regions in the dye is believed to be the reason thioflavin T binds to amyloids (*63*). Binding to the fibril fixes ThT into place, creating an increase in fluorescence. Table 4 shows the intensity of protein aggregates in the presence of Thioflavin T. Any appreciable intensity signifies the presence of amyloids, as the monomer protein gives no fluorescence signal. Interestingly, not only did the disease-causing mutants MBP-OLF display evidence of amyloids but also the SNPs, wild-type MBP-OLF, and full-length myocilin.

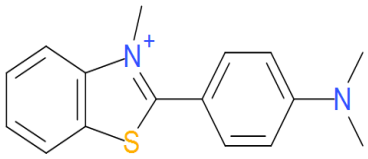

Figure 10. Structure of Thioflavin T.

Table 4. Fluorescence intensity of protein aggregates (0.25 mg/mL) in the presence of thioflavin T at 485 nm.

Protein	Intensity, 485 nm (afu)
Monomer OLF	-0.25
Wild-type	7.70
Full-Length	23.61
G246R	13.50
R272G	45.58
E323K	34.86
G326R	32.46
G364V	50.69
G367R	36.04
T377M	35.12
K423E	29.50
V426F	68.64
A427T	37.80
C433R	34.99
Y437H	20.64
A445V	40.22
P481L	54.43
I499F	52.88
S502P	57.20
N480K	43.20
N480L	158.41
E352Q	51.08
K398R	40.42
E396D	38.88

Propensity of Aggregation in Size-exclusion Chromatography

Gel filtration chromatography is an effective way to separate aggregated protein from monomeric protein (*64*). For all OLF variants studied, aggregation was observed in the void volume from gel filtration. The ratio between the aggregate and monomer peak of a given protein can give information about the propensity to aggregate when compared to other proteins. For example, in Figure 11A, wild-type MBP-OLF has a 6:4 aggregate to monomer peak ratio. However when compared to E396D, overlaid in red, wild-type has higher aggregation than the SNPs because E396D has an 8:2 monomer to aggregate ratio. The SNPs' chromatographs gave an interesting observation, implying that SNPs have a low propensity for aggregation. On the other hand, mutant MBP-OLFs gave a variety of different ratios, which can be loosely linked to the ranking of mutants in Table 3. For instance, Figure 11B shows wild-type MBP-OLF and G367R. G367R gives about a 9:1 aggregate to monomer peak and there is a high level of aggregation. When compared to wild-type, the ratio of monomer to aggregate for G367R implies a decent propensity for aggregation. However, when looking at Figure 11C, W286R gives no monomeric peak, signifying almost complete aggregation. Table 3 shows that W286R has no melting temperature, due to this issue of complete aggregation, while G367R has a medium melting temperature. Based on this information, W286R could be considered more of a severe mutation than G367R. This conclusion can give more evidence to the trend presented in Table 3.

Overall, the data present in this thesis give insight into the relationship between the genotype and phenotype of POAG. The severity of the mutation can be deduced by the melting temperature, aggregation propensity, and additional data presented in Table 3. Groups 1 and 2 would be severe while Group 3 mutants could be moderate. Finally, Group 4 mutations are either very mild or benign. Furthermore, the thermal stability assay demonstrated these mutants can be stabilized by small molecules. This assay is the beginning step in designing a high-throughput assay to identify small molecule stabilizers for myocilin. Future research can refine this assay to identify a small molecule, which can be use to stabilize myocilin, rescue the HTM cells from death and alleviate the symptoms of glaucoma.

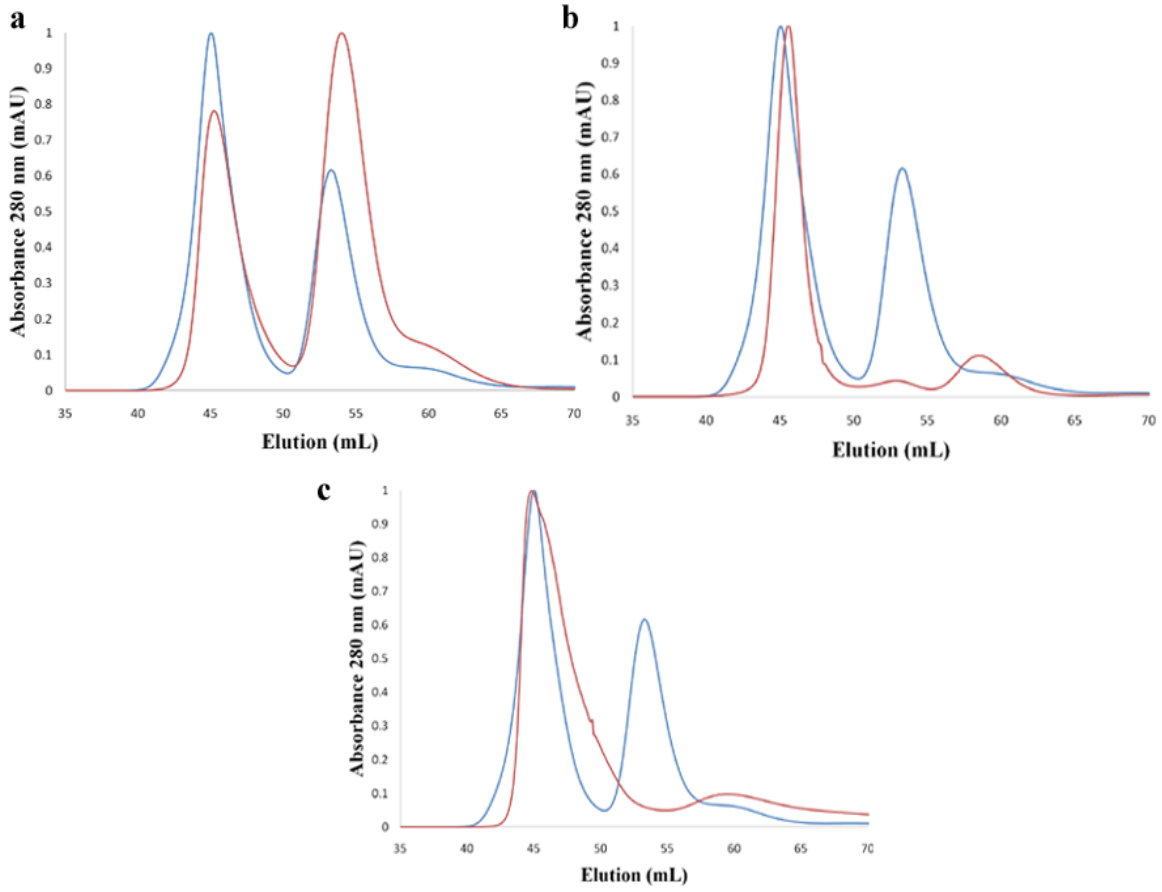

Figure 11. Size exclusion chromatography. (A) Wild-type MBP-OLF and E396D. (B) Wild-type MBP-OLF and G367R. (C) Wild-type MBP-OLF and W286R. Blue line represents wild-type and red line represents mutant protein.

CHAPTER 4

MATERIALS AND METHODS

Molecular Biology. The MYOC-OLF gene was amplified by polymerase chain reaction (5-PRIME Master Mix, Fisher Scientific) from a plasmid reported previously (*45*), annealed into the pET-30 X_a/LIC vector (Novagen), then subcloned into the pMAL-c4x vector (New England Biolabs). The final pMAL-c4x construct incorporates a 7-amino acid linker between MBP and OLF (SSSIEGR), with a Factor X_a cleavage site (IEGR). After plasmid replication in NovaBlue Gigasingles (Novagen), the plasmid was isolated (QIAPrep, Qiagen). Mutant MBP-OLFs were generated by site directed mutagenesis (QuikChange, Stratagene). Primers used for mutagenesis are listed in Appendix 1. All plasmids were verified by DNA sequencing (Operon).

Protein Expression and Purification. Wild type and mutant plasmids were transformed into Rosetta-gami 2(DE3)pLysS (Novagen) cells and cultured in Superior Broth (US Biological) to an optical density of ~0.7 at 600 nm, cooled to 18 °C, and induced with 0.5 mM isopropyl β-D-thiogalactopyranoside. After overnight growth (12–16 hours), cells were pelleted, flash frozen, and stored at –80 °C.

Cell pellets were lysed by French Press in the presence of 10 mM sodium/potassium phosphate (pH 7.2), 200 mM NaCl, 1 mM EDTA (Buffer A), supplemented with Roche Complete Protease Inhibitor. Cell debris was removed by ultracentrifugation (42000 g for 30 min) and the clarified supernatant loaded onto a 20 ml High Flow Amylose Resin (New England Biolabs) column equilibrated with Buffer A. The MBP-OLFs were eluted with Buffer A plus 10 mM maltose, concentrated using an Amicon Ultra YM-30 centrifugation device, and either flash frozen and stored at –80 °C,

or loaded on a Superdex 75 gel filtration prep grade column (GE Healthcare) equilibrated with 10 mM Phosphate (Na/K), 200 mM NaCl, pH 7.2 (Buffer B). Only those fractions corresponding to monomeric MBP-OLF were pooled for further study.

Cleavage of MBP-OLF was accomplished by overnight (~ 16 h) incubation with Factor X_a (New England Biolabs) in 50 mM Tris pH 8, 100 mM NaCl, 5 mM $CaCl_2$. Cleaved OLF was fractionated from uncleaved material and MBP by taking the flowthrough fraction from amylose resin for purification on Superdex 75. MBP used in these studies was also isolated this way. Protein in experiments was used within three days of purification. SDS-PAGE analysis was conducted as described (*65*).

Thermal Stability Assay. Sypro Orange (Invitrogen), supplied as a 5,000X solution in dimethylsulfoxide, was diluted in Buffer B (1:1000) and mixed just prior to preparing samples for the assay. Reactions of 30 μL were prepared at room temperature and delivered to 96-well optical plates (Applied Biosystems) before sealing with optical film. 3 μL of diluted Sypro Orange was added to the protein solutions ranging in concentration from 0.5–1.5 μM. Protein samples were in Buffer B. Except when indicated otherwise, maltose was present at 50 mM. Compounds tested for stability enhancement were obtained from commercial sources. Where indicated, TMAO and sarcosine were tested at 5 M in the reaction buffer, whereas 4-PBA was tested in a concentration range of 1 mM to 0.5 M. For all others, a 5 M stock was diluted to 3 M in Buffer B. Plates included a baseline control containing Sypro Orange with no protein. The pH of the final solutions did not deviate significantly from 7.

Fluorescence data were acquired on an Applied Biosciences Step-One Plus RT-PCR instrument equipped with fixed excitation wavelength (480 nm) and ROX®

emission filter (610 nm). Melting experiments were conducted from 25–95 °C with a 1 °C per min increase. No difference in T_m was observed when the rate of heating was slowed to 0.5 °C per min. No dependence of protein concentration on T_m was observed above a minimum threshold protein concentration. Data were processed using GraphPad Prism. After baseline subtraction, data were trimmed to include the boundaries and the transition of interest and normalized. The reported T_m is the inflection point of the sigmoidal curve, which was fit as described previously (*33*).

Circular Dichroism. Prior to CD scans, monomeric MBP-OLF samples were purified once more on an analytical Superdex 75 GL column (GE Healthcare) to remove all traces of aggregate or MBP and then concentrated to 0.25-0.5 μM (uncleaved protein) or 1.0-5.0 μM (cleaved protein). CD spectra were acquired at 25 °C on a Jasco J-810 CD spectropolarimeter. Twenty consecutive scans (forty for cleaved protein) ranging from 200 nm to 300 nm, using a bandwidth of 1 nm at a continuous scanning rate of 500 nm/min, were averaged for each sample.

Thioflavin T. The presence of amyloid fibrils was determined using a fluorescence dye thioflavin T. A stock solution of thioflavin T was prepared by dilution in deionized water to 1 mg/mL. Thioflavin T was further diluted to 5 μM in Buffer A with 0.25 mg/mL aggregate protein (taken from void volume of gel filtration purification). Fluorescence emission spectra of thioflavin T-protein complex were recorded using excitation and emission wavelengths of 412 and 430-600 nm respectively, using a Shimadzu RF-5301 PC spectrofluorophotometer. The average of three intensities was reported at 485 nm.

In-gel trypsin digest and mass spectroscopy (MALDI-TOF/MS) analysis.

Full-length myocilin was excised from a SDS-PAGE and acetonitrile was added to dehydrate the gel pieces. Ten mM dithiotreitol (DTT) in 100 mM ammonium bicarbonate was added after removal of the acetonitrile. The solution was incubated for an hour at 56 °C and then with the removal of the DTT solution, 55 mM iodoacetamide in 100 mM ammonium bicarbonate was added. Incubated for 45 minutes in the dark, the gel pieces were vortexed every 15 minutes. The iodoacetamide solution was replaced with 100 mM ammonium bicarbonate and then with acetonitrile to dehydrate the gel pieces. This process was repeated three times. After the final dehydration, the gel pieces were dried with a speed-vac and rehydrated with the digestion buffer (50 mM ammonium bicarbonate, 5 mM calcium chloride, and 12.5 ng/μL trypsin (Promega, mass spectrometry grade)). After incubation in an ice bath for 45 minutes, this solution was replaced with digestion buffer without trypsin and incubated overnight at 37 °C. Twenty mM ammonium bicarbonate followed by three cycles of 5% formic acid in 50% acetonitrile was performed to extract the digested peptides from the gel pieces (*66*). The combined extractions were dried in a speed-vac and submitted to the Georgia Institute of Technology Bioanalytical Mass Spectrometry Facility for peptide mass fingerprinting analysis. Spectra were acquired on a MALDI-TOF/TOF tandem mass spectrometer, Applied Biosystems 4700 Proteomics Analyzer. All peaks were deisotoped and analyzed by GPS Explorer (Applied Biosystems) software, specifically the MASCOT program. The National Center for Biotechnology non-redundant (NCBInr) database was searched with the following parameters: *homo sapiens* as taxonomy; trypsin as the enzyme; up to one missed cleavage; precursor tolerance of 75 ppm; peptide charge of 1^+; and

monoisotopic. Only peaks with a minimum 3:1 signal-to-noise ratio are reported in Table 1.

APPENDIX I

LIST OF PRIMERS

Plasmid Template	Target vector		Primer Used
			Myocilin-OLF cloning
pcDNA	pET-30XaLIC	Forward	5’-GGTATTGAGGGTCGCTTGAAGGAGAGCCCATCTG
		Reverse	5’-AGAGGAGAGTTAGAGCCTTATCACATCTTGGAGAGCTTGATG
pET-30XaLIC	pMAL-c4x	Forward	5’-CGCCGAGCTCTATTGAGGGTCGC
		Reverse	5’-GCCGAATTCAGGAGAGTTAGAGCCTTATCA
			Full-length myocilin cloning
pET-30XaLIC	pMAL-c4x	Forward	5’-ATCGGATCCAGGACAGCTCAGCTCAGG
		Reverse	5’-GCCGAATTCTTATCACATCTTGGAGAGCTTGAT
			Mutagenesis
D380A			5’-GCTACACGGACATTGCCTTGGCTGTGGATG
I477S			5’-GTACAGCAGCATGTCTGACTACAACCCCCTCG
I477N			5’-GTACAGCAGCATGAATGACTACAACCCCCTGG
K423E			5’-GGGAGACAAACATCCGTGAACAGTCAGTCGCCAATGCC
T377M			5'-GTATTCTTGGGGTGGCTACATGGACATTGACTTGGCTGTG
A427T			5'-CATCCGTAAGCAGTCAGTCACCAATGCCTTCATCATCTG
C433R			5'-CAATGCCTTCATCATCCGTGGCACCTTGTACACC
I499F			5'-GAACATGGTCACTTATGACTTCAAGCTTTCCAAGATGTG
Y437H			5'-CATCTGTGGCACCTTGCACACCGTCAGCAGCTAC
P481L			5'-GCATGATTGACTACAACCTGCTGGAGAAGAAGCTCTTTG
R272G			5'-CAAGTATGGTGTGTGGATGGGAGACCCCAAGCCCACCTAC
N480K			5'-GCATGATTGACTACAAGCCCCTGGAGAAGAAGC

Plasmid Template	Target vector	Primer Used
N480L		5'-CAGCAGCATGATTGACTACCTACCCCTGGAGAAGAAGCTC
S502P		5'-CACTTATGACATCAAGCTTCCCAAGATGTGATAAGGCTC
G364V		5'-GAAATCCCTGGAGCTGTCTACCACGGACAGTTC
G367R		5'-GGAGCTGGCTACCACAGACAGTTCCCGTATTC
A445V		5'-GCAGCTACACCTCAGTAGATGCTACCGTCAAC
E323K		5’-CATACTGCCTAGGCCACTGAAAAGCACGGGTGCTGTGG
V426F		5'-CAAACATCCGTAAGCAGTCATTCGCCAATGCCTTCATCATC
G252R		5'-GAACTAGTTTGGGTAAGAGAGCCTCTCACGC
G246R		5'-GGAGACACCGGATGTAGAGAACTAGTTTGGG
G326R		5'-CCACTGGAAAGCACGCGTGCTGTGGTGTAC
W286R		5'-CCCAGGAGACCACGAGGAGAATCGACACAG
K398R		5’-CGATGAGGCCAGAGGTGCCATTGTCCTCTC
E396D		5'-CATTTACAGCACCGATGACGCCAAAGGTGCCATTGTC
E352Q		5'-GATATGAGCTGAATACCCAGACAGTGAAGGCTGAG

REFERENCES

1. Kwon, Y. H., Fingert, J. H., Kuehn, M. H., and Alward, W. L. (2009) Primary open-angle glaucoma, *N Engl J Med 360*, 1113-1124.

2. Alward, W. L. (1998) Medical management of glaucoma, *N Engl J Med 339*, 1298-1307.

3. Resch, Z. T., and Fautsch, M. P. (2009) Glaucoma-associated myocilin: A better understanding but much more to learn, *Experimental Eye Research 88*, 704-712.

4. Wentz-Hunter, K., Kubota, R., Shen, X., and Yue, B. Y. (2004) Extracellular myocilin affects activity of human trabecular meshwork cells, *J Cell Physiol 200*, 45-52.

5. Fautsch, M. P., and Johnson, D. H. (2001) Characterization of myocilin-myocilin interactions, *Invest Ophthalmol Vis Sci 42*, 2324-2331.

6. Filla, M. S., Liu, X., Nguyen, T. D., Polansky, J. R., Brandt, C. R., Kaufman, P. L., and Peters, D. M. (2002) In vitro localization of TIGR/MYOC in trabecular meshwork extracellular matrix and binding to fibronectin, *Invest Ophthalmol Vis Sci 43*, 151-161.

7. Goldwich, A., Scholz, M., and Tamm, E. R. (2009) Myocilin promotes substrate adhesion, spreading and formation of focal contacts in podocytes and mesangial cells, *Histochemistry and Cell Biology 131*, 167-180.

8. Tomarev, S. I., and Nakaya, N. (2009) Olfactomedin domain-containing proteins: possible mechanisms of action and functions in normal development and pathology, *Mol Neurobiol 40*, 122-138.

9. Gobeil, S., Letartre, L., and Raymond, V. (2006) Functional analysis of the glaucoma-causing TIGR/myocilin protein: Integrity of amino-terminal coiled-coil regions and olfactomedin homology domain is essential for extracellular adhesion and secretion, *Experimental Eye Research 82*, 1017-1029.

10. Joe, M. K., Sohn, S., Hur, W., Moon, Y., Choi, Y. R., and Kee, C. (2003) Accumulation of mutant myocilins in ER leads to ER stress and potential

cytotoxicity in human trabecular meshwork cells, *Biochem Biophys Res Commun 312*, 592-600.

11. Liu, Y., and Vollrath, D. (2004) Reversal of mutant myocilin non-secretion and cell killing: implications for glaucoma, *Hum Mol Genet 13*, 1193-1204.

12. Vollrath, D., and Liu, Y. H. (2006) Temperature sensitive secretion of mutant myocilins, *Experimental Eye Research 82*, 1030-1036.

13. Kim, B. S., Savinova, O. V., Reedy, M. V., Martin, J., Lun, Y., Gan, L., Smith, R. S., Tomarev, S. I., John, S. W., and Johnson, R. L. (2001) Targeted Disruption of the Myocilin Gene (Myoc) Suggests that Human Glaucoma-Causing Mutations Are Gain of Function, *Mol Cell Biol 21*, 7707-7713.

14. Lam, D. S., Leung, Y. F., Chua, J. K., Baum, L., Fan, D. S., Choy, K. W., and Pang, C. P. (2000) Truncations in the TIGR gene in individuals with and without primary open-angle glaucoma, *Invest Ophthalmol Vis Sci 41*, 1386-1391.

15. Ellgaard, L., and Helenius, A. (2003) Quality control in the endoplasmic reticulum, *Nat Rev Mol Cell Biol 4*, 181-191.

16. Carbone, M. A., Ayroles, J. F., Yamamoto, A., Morozova, T. V., West, S. A., Magwire, M. M., Mackay, T. F. C., and Anholt, R. R. H. (2009) Overexpression of Myocilin in the Drosophila Eye Activates the Unfolded Protein Response: Implications for Glaucoma, *Plos One 4*.

17. Wang, L., Zhuo, Y., Liu, B., Huang, S., Hou, F., and Ge, J. (2007) Pro370Leu mutant myocilin disturbs the endoplasm reticulum stress response and mitochondrial membrane potential in human trabecular meshwork cells, *Mol Vis 13*, 618-625.

18. Yam, G. H. F., Gaplovska-Kysela, K., Zuber, C., and Roth, J. (2007) Aggregated myocilin induces Russell bodies and causes apoptosis - Implications for the pathogenesis of myocilin-caused primary open-angle glaucoma, *American Journal of Pathology 170*, 100-109.

19. Powers, E. T., Morimoto, R. I., Dillin, A., Kelly, J. W., and Balch, W. E. (2009) Biological and Chemical Approaches to Diseases of Proteostasis Deficiency, *Annual Review of Biochemistry 78*, 959-991.

20. Cohen, F. E., and Kelly, J. W. (2003) Therapeutic approaches to protein-misfolding diseases, *Nature 426*, 905-909.

21. Nagy, I., Trexler, M., and Patthy, L. (2003) Expression and characterization of the olfactomedin domain of human myocilin, *Biochemical and Biophysical Research Communications 302*, 554-561.

22. Pandaranayaka, P. J. E., Kanagavalli, J., Krishnadas, S. R., Sundaresan, P., and Krishnaswamy, S. (2008) Over expression and purification of recombinant human myocilin, *World Journal of Microbiology & Biotechnology 24*, 903-907.

23. Park, B. C., Shen, X., Fautsch, M., Tibudan, M., Johnson, D., and Yue, B. (2006) Optimized bacterial expression of myocilin proteins and functional comparison of bacterial and eukaryotic myocilins, *Molecular Vision 12*, 832-840.

24. Peters, D. M., Herbert, K., Biddick, B., and Peterson, J. A. (2005) Myocilin binding to Hep II domain of fibronectin inhibits cell spreading and incorporation of paxillin into focal adhesions, *Experimental Cell Research 303*, 218-228.

25. di Guan, C., Li, P., Riggs, P. D., and Inouye, H. (1988) Vectors that facilitate the expression and purification of foreign peptides in Escherichia coli by fusion to maltose-binding protein, *Gene 67*, 21-30.

26. Burns, J. N., Orwig, S. D., Harris, J. L., Watkins, J. D., Vollrath, D., and Lieberman, R. L. (2010) Rescue of glaucoma-causing mutant myocilin thermal stability by chemical chaperones, *ACS Chem Biol 5*, 477-487.

27. Yam, G. H. T., Gaplovska-Kysela, K., Zuber, C., and Roth, J. (2007) Sodium 4-phenylbutyrate acts as a chemical chaperone on misfolded myocilin to rescue cells from endoplasmic reticulum stress and apoptosis, *Investigative Ophthalmology & Visual Science 48*, 1683-1690.

28. Trovato, A., Seno, F., and Tosatto, S. C. E. (2007) The PASTA server for protein aggregation prediction, *Protein Engineering Design & Selection 20*, 521-523.

29. Barnes, M. R. (2010) Genetic variation analysis for biomedical researchers: a primer, *Methods Mol Biol 628*, 1-20.

30. Database of Single Nucleotide Polymorphisms (dbSNP), National Center for Biotechnology Information, National Library of Medicine, Bethesda, MD.

31. Linhardt, R. J. (2003) 2003 Claude S. Hudson Award address in carbohydrate chemistry. Heparin: Structure and activity, *Journal of Medicinal Chemistry 46*, 2551-2564.

32. Lodish, H., Berk, A., Kaiser, C. A., Krieger, M., Scott, M. P., Bretscher, A., Ploegh, H., and Matsudaria, P. (2008) *Molecular Cell Biology*, 2nd ed., W.H. Freeman and Company, New York, NY.

33. Niesen, F. H., Berglund, H., and Vedadi, M. (2007) The use of differential scanning fluorimetry to detect ligand interactions that promote protein stability, *Nature Protocols 2*, 2212-2221.

34. Waldron, T. T., and Murphy, K. P. (2003) Stabilization of proteins by ligand binding: Application to drug screening and determination of unfolding energetics, *Biochemistry 42*, 5058-5064.

35. Lieberman, R. L., D'Aquino, J. A., Ringe, D., and Petsko, G. A. (2009) Effects of pH and Iminosugar Pharmacological Chaperones on Lysosomal Glycosidase Structure and Stability, *Biochemistry 48*, 4816-4827.

36. Loo, T. W., Bartlett, M. C., and Clarke, D. M. (2008) Correctors promote folding of the CFTR in the endoplasmic reticulum, *Biochemical Journal 413*, 29-36.

37. Rosenbluth, R. F., and Fatt, I. (1977) TEMPERATURE-MEASUREMENTS IN EYE, *Experimental Eye Research 25*, 325-341.

38. Sawkar, A. R., Schmitz, M., Zimmer, K. P., Reczek, D., Edmunds, T., Balch, W. E., and Kelly, J. W. (2006) Chemical chaperones and permissive temperatures atter the cellular locatization of Gaucher disease associated glucocerebrosidase variants, *Acs Chemical Biology 1*, 235-251.

39. Balch, W. E., Morimoto, R. I., Dillin, A., and Kelly, J. W. (2008) Adapting proteostasis for disease intervention, *Science 319*, 916-919.

40. Arakawa, T., Ejima, D., Kita, Y., and Tsumoto, K. (2006) Small molecule pharmacological chaperones: From thermodynamic stabilization to

pharmaceutical drugs, *Biochimica Et Biophysica Acta-Proteins and Proteomics 1764*, 1677-1687.

41. Arakawa, T., and Timasheff, S. N. (1985) THE STABILIZATION OF PROTEINS BY OSMOLYTES, *Biophysical Journal 47*, 411-414.

42. Bolen, D. W., and Baskakov, I. V. (2001) The osmophobic effect: Natural selection of a thermodynamic force in protein folding, *Journal of Molecular Biology 310*, 955-963.

43. Bolen, D. W., and Rose, G. D. (2008) Structure and energetics of the hydrogen-bonded backbone in protein folding, *Annual Review of Biochemistry 77*, 339-362.

44. Shimizu, S., Lichter, P. R., Johnson, A. T., Zhou, Z. H., Higashi, M., Gottfredsdottir, M., Othman, M., Moroi, S. E., Rozsa, F. W., Schertzer, R. M., Clarke, M. S., Schwartz, A. L., Downs, C. A., Vollrath, D., and Richards, J. E. (2000) Age-dependent prevalence of mutations at the GLC1A locus in primary open-angle glaucoma, *American Journal of Ophthalmology 130*, 165-177.

45. Vollrath, D., and Zhou, Z. (1999) A cellular assay distinguishes normal and mutant TIGR/myocilin protein, *American Journal of Human Genetics 65*, 604.

46. Adam, M. F., Belmouden, A., Binisti, P., Brezin, A. P., Valtot, F., Bechetoille, A., Dascotte, J. C., Copin, B., Gomez, T., Chaventre, A., Bach, J. F., and Garchon, H. J. (1997) Recurrent mutations in a single exon encoding the evolutionarily conserved olfactomedin-homology domain of TIGR in familial open-angle glaucoma, *Human Molecular Genetics 6*, 2091-2097.

47. Alward, W. L. M., Fingert, J. H., Coote, M. A., Johnson, A. T., Lerner, S. F., Junqua, D., Durcan, F. J., McCartney, P. J., Mackey, D. A., Sheffield, V. C., and Stone, E. M. (1998) Clinical features associated with mutations in the chromosome 1 open-angle glaucoma gene (GLCIA), *New England Journal of Medicine 338*, 1022-1027.

48. Brezin, A. P., Bechetoille, A., Hamard, P., Valtot, F., Berkani, M., Belmouden, A., Adam, M. F., deDinechin, S. D., Bach, J. F., and Garchon, H. J. (1997) Genetic heterogeneity of primary open angle glaucoma and ocular hypertension: Linkage to GLC1A associated with an increased risk of severe glaucomatous optic neuropathy, *Journal of Medical Genetics 34*, 546-552.

49. Bruttini, M., Longo, I., Frezzotti, P., Ciappetta, R., Randazzo, A., Orzalesi, N., Fumagalli, E., Caporossi, A., Frezzotti, R., and Renieri, A. (2003) Mutations in the myocilin gene in families with primary open-angle glaucoma and juvenile open-angle glaucoma, *Archives of Ophthalmology 121*, 1034-1038.

50. Faucher, M., Anctil, J. L., Rodrigue, M. A., Duchesne, A., Bergeron, D., Cote, G., Arsenault, R., Bergeron, J., Morissette, J., and Raymond, V. (2002) Founder mutations for glaucoma caused by TIGR/myocilin in the Quebec population, *Investigative Ophthalmology & Visual Science 43*, 3390.

51. Fingert, J. H., Heon, E., Liebmann, J. M., Yamamoto, T., Craig, J. E., Rait, J., Kawase, K., Hoh, S. T., Buys, Y. M., Dickinson, J., Hockey, R. R., Williams-Lyn, D., Trope, G., Kitazawa, Y., Ritch, R., Mackey, D. A., Alward, W. L. N., Sheffield, V. C., and Stone, E. M. (1999) Analysis of myocilin mutations in 1703 glaucoma patients from five different populations, *Human Molecular Genetics 8*, 899-905.

52. Hulsman, C. A. A., de Jong, P., Lettink, M., van Duijn, C. M., Hofman, A., and Bergen, A. A. B. (2002) Myocilin mutations in a population-based sample of cases with open-angle glaucoma: the Rotterdam Study, *Graefes Archive for Clinical and Experimental Ophthalmology 240*, 468-474.

53. Kanagavalli, J., Krishnadas, S. R., Pandaranayaka, E., Krishnaswamy, S., and Sundaresan, P. (2003) Evaluation and understanding of myocilin mutations in Indian primary open angle glaucoma patients, *Molecular Vision 9*, 606-614.

54. Mackey, D. A., Healey, D. L., Fingert, J. H., Coote, M. A., Wong, T. L., Wilkinson, C. H., McCartney, P. J., Rait, J. L., de Graaf, A. P., Stone, E. M., and Craig, J. E. (2003) Glaucoma phenotype in pedigrees with the myocilin Thr377Met mutation, *Arch Ophthalmol 121*, 1172-1180.

55. Melki, R., Belmouden, A., Brezin, A., and Garchon, H. J. (2003) Myocilin analysis by DHPLC in French POAG patients: increased prevalence of Q368X mutation, *Hum Mutat 22*, 179.

56. Morissette, J., Clepet, C., Moisan, S., Dubois, S., Winstall, E., Vermeeren, D., Nguyen, T. D., Polansky, J. R., Cote, G., Anctil, J. L., Amyot, M., Plante, M., Falardeau, P., and Raymond, V. (1998) Homozygotes carrying an autosomal dominant TIGR mutation do not manifest glaucoma, *Nature Genetics 19*, 319-321.

57. Richards, J. E., Ritch, R., Lichter, P. R., Rozsa, F. W., Stringham, H. M., Caronia, R. M., Johnson, D., Abundo, G. P., Willcockson, J., Downs, C. A., Thompson, D. A., Musarella, M. A., Gupta, N., Othman, M. I., Torrez, D. M., Herman, S. B., Wong, D. J., Higashi, M., and Boehnke, M. (1998) Novel trabecular meshwork inducible glucocorticoid response mutation in an eight-generation juvenile-onset primary open-angle glaucoma pedigree, *Ophthalmology 105*, 1698-1707.

58. Rozsa, F. W., Shimizu, S., Lichter, P. R., Johnson, A. T., Othman, M. I., Scott, K., Downs, C. A., Nguyen, T. D., Polansky, J., and Richards, J. E. (1998) GLC1A mutations point to regions of potential functional importance on the TIGR/MYOC protein, *Mol Vis 4*, 20.

59. Stoilova, D., Child, A., Brice, G., Desai, T., Barsoum-Homsy, M., Ozdemir, N., Chevrette, L., Adam, M. F., Garchon, H. J., Crick, R. P., and Sarfarazi, M. (1998) Novel TIGR/MYOC mutations in families with juvenile onset primary open angle glaucoma, *Journal of Medical Genetics 35*, 989-992.

60. Vasconcellos, J. P., Melo, M. B., Costa, V. P., Tsukumo, D. M., Basseres, D. S., Bordin, S., Saad, S. T., and Costa, F. F. (2000) Novel mutation in the MYOC gene in primary open glaucoma patients, *J Med Genet 37*, 301-303.

61. Kelly, S. M., Jess, T. J., and Price, N. C. (2005) How to study proteins by circular dichroism, *Biochimica Et Biophysica Acta-Proteins and Proteomics 1751*, 119-139.

62. Van Holde, K. E., Johnson, W. C., and Ho, P. S. (2006) *Principles of Physical Biochemistry*, 6th ed., Pearson Education, Inc., Upper Saddle Valley, NJ.

63. Khurana, R., Coleman, C., Ionescu-Zanetti, C., Carter, S. A., Krishna, V., Grover, R. K., Roy, R., and Singh, S. (2005) Mechanism of thioflavin T binding to amyloid fibrils, *Journal of Structural Biology 151*, 229-238.

64. Kunji, E. R. S., Harding, M., Butler, P. J. G., and Akamine, P. (2008) Determination of the molecular mass and dimensions of membrane proteins by size exclusion chromatography, *Methods 46*, 62-72.

65. Sambrook, J., and Russell, D. W. (2001) *Molecular Cloning: a laboratory manual*, 3rd ed., Cold Spring Harbor Laboratory Press, Cold Spring Harbor, NY.

66. Shevchenko, A., Wilm, M., Vorm, O., and Mann, M. (1996) Mass spectrometric sequencing of proteins silver-stained polyacrylamide gels, *Anal Chem 68*, 850-858.